



## NIRSpec Technical Note NTN-2012-008

Author(s): S. Birkmann  
Date of Issue: August 3, 2012  
Version: 1.0

# The radiometric stability of the RCSS based on telemetry data

## Abstract:

This document assesses the radiometric stability of the RCSS based on cycle 1 telemetry data. We briefly describe the format of the used telemetry data and its origin. We find that, integrated over the  $\sim 1$  to  $\sim 1.9 \mu\text{m}$  wavelength range, the RCSS is stable to  $10^{-3}$  on time scales of hours. Furthermore, the observed drifts can be well modeled by an exponential function with root mean square residuals typically better than  $10^{-4}$ . Based on the findings in this note we recommend to use the high resolution Band I grating with the RCSS IFS3\_N source for the simulation of exoplanet transit observations.

## 1 INTRODUCTION

The Radiometrically Calibrated Spectral Source (RCSS) is one of NIRSpec's on-ground calibration sources (see Birkmann 2011 for an overview of NIRSpec's optical ground support equipment). It consists of a small gold-coated integrating sphere with six redundant continuum light sources and a pinhole at the sphere exit. This pinhole is imaged by a telescope of an Offner design that mimics the JWST telescope's  $f/20$ -beam and pupil, and supplies a point source to the instrument. A more detailed description is available in the RCSS user manual (Kochems 2010).

The patrol range of the RCSS is limited to an area close to the fixed slits in NIRSpec. Its main use is to measure the slit and diffraction losses of NIRSpec's spectroscopic modes, but it can also be used to simulate exoplanet transit observations through the S1600 slit. Such measurements are planned for the second performance verification and calibration campaign scheduled to start late 2012. The scope of this document is to assess the radiometric stability of the RCSS from telemetry data obtained during the first NIRSpec calibration campaign conducted in early 2011. This data will help us to determine what stability can be expected and which wavelength range should be preferred when planning the exoplanet transit simulation observations.

## 2 THE TELEMETRY DATA

During each NIRSpec observation, a stream of telemetry of instrument and ground support equipment readings is recorded. This stream is written as a list of comma separated values (csv) into the same directory as the fits data associated with the exposure. Each entry contains a time stamp, the keyword of the telemetry taken, the actual value, and some additional information irrelevant for this technical note. Typical sampling cadences range from one to several seconds, depending on the type of telemetry data and its origin (instrument or GSE). The RCSS contains three detector diodes that are located in the integrating sphere:

1. Si diode,  $1.1 \times 1.1 \text{ mm}^2$ , from Hamamatsu
2. InGaAs diode, 1.0 mm diameter, from Judson
3. InSb diode, 1.0 mm diameter, from Hamamatsu

All three detectors are bare, i.e. there is no window or filter in front of the light sensitive area. The cut-off wavelengths for the detector diodes (50% of the peak response) is about  $0.9 \mu\text{m}$  for the Silicon,  $1.9 \mu\text{m}$  for the InGaAs, and  $5.5 \mu\text{m}$  for the InSb diode. The (photo)current is measured by three Picoammeters from Keithley (Model 6485,  $5\frac{1}{2}$  digit resolution) and recorded approximately every ten seconds in the telemetry stream (in Ampere). The associated keywords are GNRS\_RCS\_IOUT\_DET#, where # is to be replaced with a number from 1 to 3 giving the detector number as in the list above.

The RCSS filaments are current driven with either 10 mA or 17 mA, depending on the illumination mode chosen. The voltage across the active filament is also recorded in the telemetry (in Volts), as is the resistance (in Ohms). The corresponding keywords are GNRS\_RCS\_LAMP#\_V and GNRS\_RCS\_LAMP#\_R for voltage and resistance, respectively, and # replaced by either A or B giving the active lamp (nominal/redundant). See table 1 for a summary of available RCSS modes and their active lamps.

## 3 RADIOMETRIC STABILITY

There was no dedicated test of the RCSS radiometric stability during the cycle 1 calibration campaign and thus there is no NIRSpec data that is suited to assess the stability of the RCSS. Although there are a few cases where the RCSS was operated in the same mode for longer periods, the conditions presented to NIRSpec always changed, i.e. the source was moved and/or the PSF changed due to an RMA focus sweep.

The radiometric stability is therefore assessed based on the telemetry readings of the three photodiodes and the filament resistance. We have selected a few cases where the RCSS was on in the same mode for a significant time (several minutes to hours). Examples for this are the PREP-RCSS-SEARCH and IMA\_PSF test sequences. Table 2 summarizes the data used for this technical note.

In Figs. 1 to 3 we show the diode readings obtained for the three NID ranges listed in table 2. In each figure, measurements are shown by the diamond symbols. The second y-axis on the right side gives the relative signal (diode current divided by mean of the diode current) and the dashed line shows the mean current.

RCSS mode	Lamp		Current [mA]	Aperture [mm]	Comment
	A	B			
MOS1_N	2		17	1.39	MOS Band I nominal
MOS1_R		2	17	1.39	MOS Band I redundant
MOS2_N	5		10	3.47	MOS Band II nominal
MOS2_R		5	10	3.47	MOS Band II redundant
MOS3_N	5		10	3.47	MOS Band III nominal
MOS3_R		5	10	3.47	MOS Band III redundant
MOSBB_N	3		10	0.52	MOS PRISM nominal
MOSBB_R		3	10	0.52	MOS PRISM redundant
IFS1_N		1	17	2.64	IFU Band I nominal
IFS1_R	1		17	2.64	IFU Band I redundant
IFS2_N		1	17	2.64	IFU Band II nominal
IFS2_R	1		17	2.64	IFU Band II redundant
IFS3_N	6		17	6.00	IFU Band III nominal
IFS3_R		6	17	6.00	IFU Band III redundant

**Table 1:** List of the available RCSS modes and their used telescopes/lamps combinations. Current is the set drive current for the lamp and aperture gives the exit aperture of the telescope. Only five of the six available telescopes are actually used. Also note that the nominal lamp for IFS1 and IFS2 is B, whereas in all other cases the nominal lamp is A.

OBS_ID root	NID range	RCSS mode	Comment
PREP-RCSS-SEARCH	4579 - 4597	IFS1_N	Lamp was off for the exposure with NID=4588
IMA-PSF	5454 - 5488	MOS1_N	Sequence was interrupted after NID=5488, data quality not affected
IMA-PSF	5820 - 5934	MOSBB_N	InSb diode signal noisy due to low flux levels

**Table 2:** List of the data used to assess the RCSS radiometric stability.

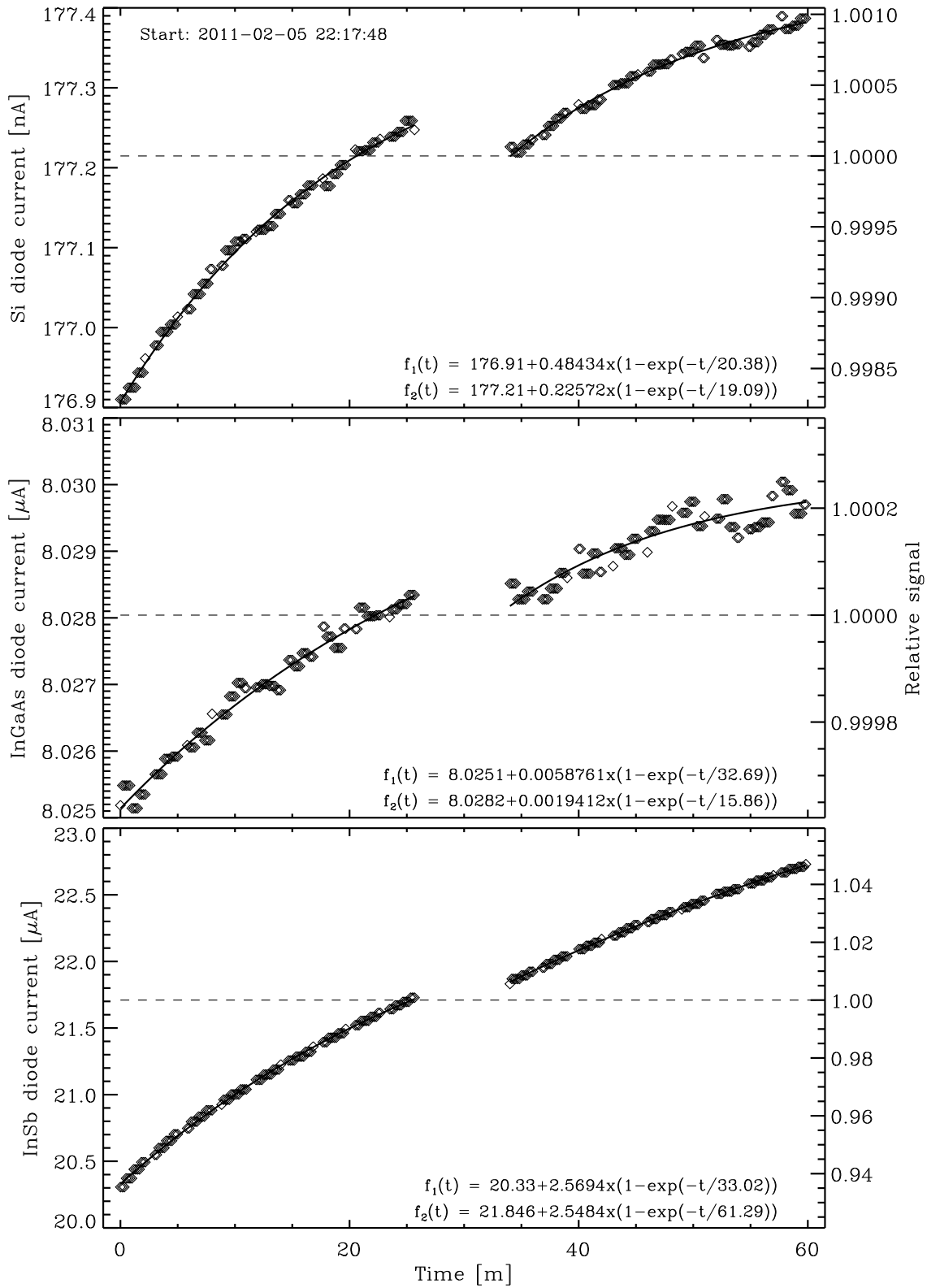


Figure 1: Measured RCSS diode currents with the IFS1\_N source on during the PREP\_RCSS\_SEARCH test sequence.

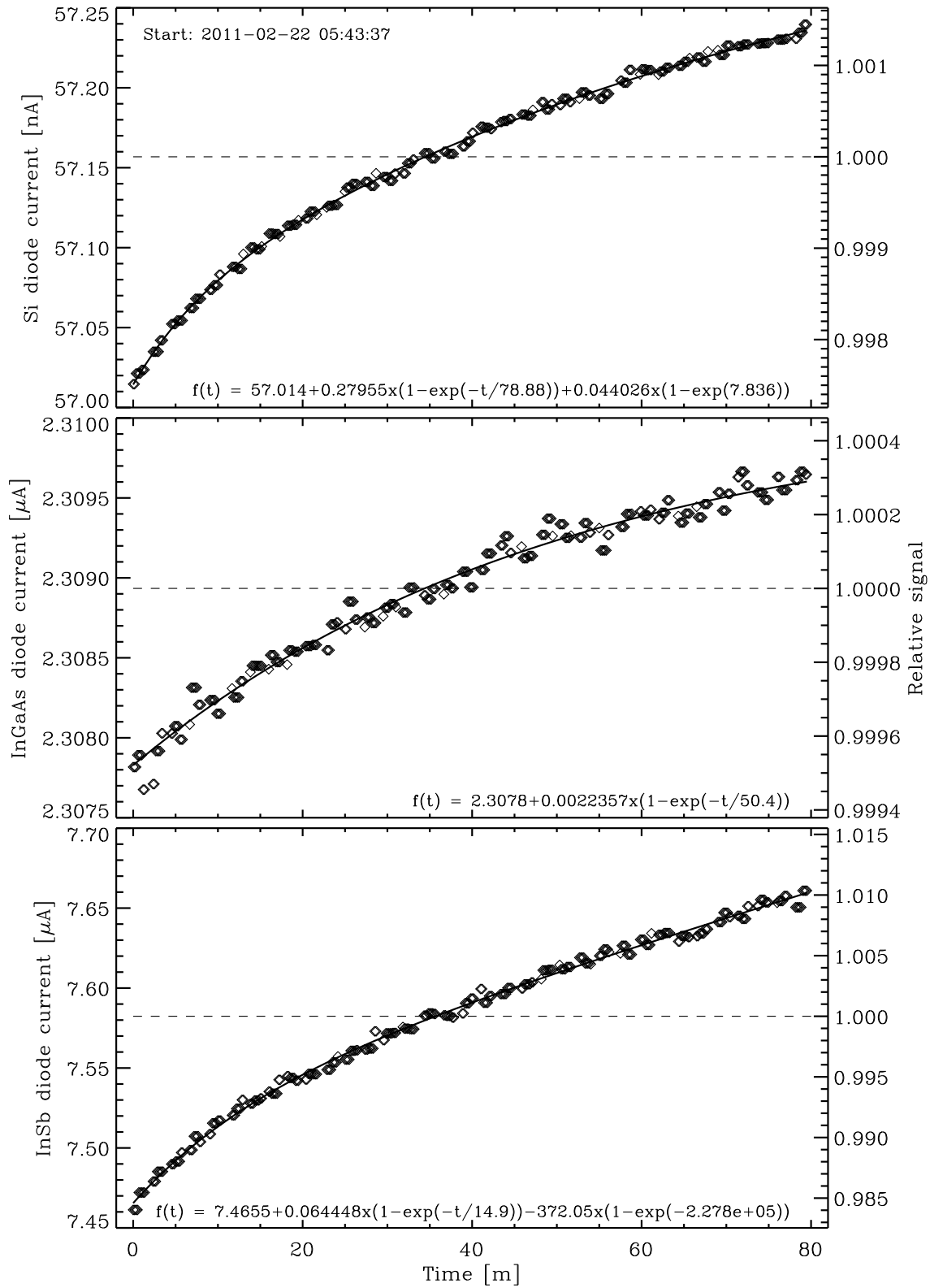


Figure 2: Measured RCSS diode currents with the MOS1\_N source on during the first run of the IMA\_PSF test sequence.

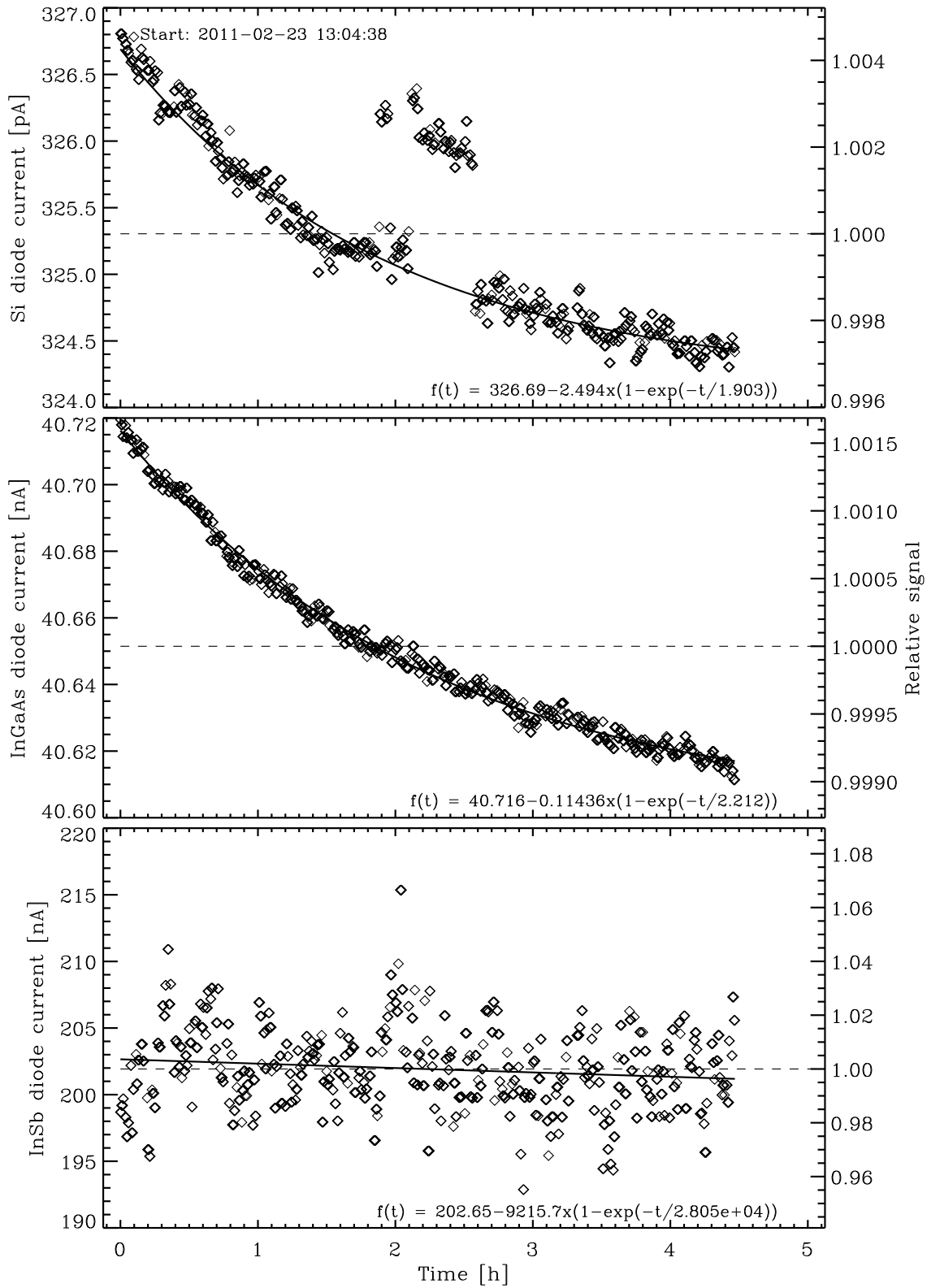


Figure 3: Measured RCSS diode currents with the MOSBB\_N source on during the second run of the IMA\_PSF test sequence.

In each case the observed signal is well described by an exponential function with one or two components of the form:

$$f(t) = P_1 + P_2 \times \left(1 - \exp\left(\frac{-t}{P_3}\right)\right) \left[+P_4 \times \left(1 - \exp\left(\frac{-t}{P_5}\right)\right)\right], \quad (1)$$

where  $P_{1...3[5]}$  are the parameters and  $t$  is the time. The part in square brackets is optional and was only used to fit the Si and InSb diode data in Fig. 2. Note that above function can also describe a linear relationship when the parameter inside the exponential becomes large compared to the time span covered by the data, i.e. when  $P_{3/5} \gg \max(t)$ . In the figures the fit is displayed as a solid line.

Fig. 1 shows the data obtained during the PREP-RCSS-SEARCH test sequence. The gap in the middle is due to the RCSS being briefly switched off, therefore the diode currents are close to zero and not visible on the plot. We fitted two functions as given in equation (1), one before and one after the break.

In Fig. 2 we present the data of the first run of the IMA-PSF sequence using the MOS1\_N lamp of the RCSS. This sequence was interrupted because the selected lamp was too bright, but it still yielded useful data for assessing the RCSS stability. Here, a five parameter fit gives significantly better results for the Si and InSb diode data, while the InGaAs readings are well fitted with the three parameter exponential. For the Si diode current the fit suggests the presence of a fast and slow exponential component, while for the InSb diode a fast and a linear component are present.

Fig. 3 shows the data obtained during the re-run of the IMA-PSF test sequence with the MOSBB\_N lamp of the RCSS. This test is by far the longest with continuous RCSS operation, about 4.5 hours. This time, the change of the diode readings is in the opposite direction, but still well described by equation (1). Due to the low flux levels (MOSBB\_1 is by far the faintest RCSS source) and the fact that the InSb diode is always read in the 2 mA range of the Keithley Picoammeter, whereas the other two diodes are read with automatically selected ranges, the signal of the InSb diode is dominated by read noise and best fitted by a linear curve. The Si diode readings show an excursion of about 1 pA for approximately 40 minutes starting roughly 1.8 hours into the test. Since this jump is not seen in the other two diodes we assume that the readings are due to some event that is not related to the filament itself, but rather the measuring device.

In table 3 we summarize the measured signal changes of each detector diode for the three NID ranges that we looked at. In all cases, drifts in the diode currents are clearly detected. For the Si and, in particular, the InGaAs detectors the observed drift is small, less than  $\pm 0.5\%$  around the mean value during the 1 to 4.5 hours of testing. The drift observed in the InSb diode is significantly larger, reaching  $\pm 7\%$ . In general, the InGaAs diode shows the best stability with excursions of less than  $\pm 0.2\%$  during the MOSBB\_N test and less than  $\pm 0.05\%$  for the two brighter RCSS lamps.

Furthermore, the measured diode currents can be well modeled using equation (1) and the root mean square (RMS) after subtracting the fit is typically better than  $1 \times 10^{-4}$  (0.01 %) for the Si and InGaAs diodes. For the high signal cases of IFS1\_N and MOS1\_N, the RMS is even

RCSS mode	Diode	Relative signal change			fit RMS
		min	max	RMS	
IFS1_N	Si	$-1.72 \times 10^{-3}$	$+9.86 \times 10^{-4}$	$7.29 \times 10^{-4}$	$3.30 \times 10^{-5}$
	InGaAs	$-3.61 \times 10^{-4}$	$+2.49 \times 10^{-4}$	$1.68 \times 10^{-4}$	$2.08 \times 10^{-5}$
	InSb	$-6.46 \times 10^{-2}$	$+4.70 \times 10^{-2}$	$3.21 \times 10^{-2}$	$5.47 \times 10^{-4}$
MOS1_N	Si	$-2.49 \times 10^{-3}$	$+1.45 \times 10^{-3}$	$1.03 \times 10^{-3}$	$4.42 \times 10^{-5}$
	InGaAs	$-5.45 \times 10^{-4}$	$+3.17 \times 10^{-4}$	$2.22 \times 10^{-4}$	$3.06 \times 10^{-5}$
	InSb	$-1.60 \times 10^{-2}$	$+1.04 \times 10^{-2}$	$6.89 \times 10^{-3}$	$4.01 \times 10^{-4}$
MOSBB_N	Si	$-3.08 \times 10^{-3}$	$+4.62 \times 10^{-3}$	$2.16 \times 10^{-3}$	$2.98 \times 10^{-4}$
	InGaAs	$-9.86 \times 10^{-4}$	$+1.67 \times 10^{-3}$	$6.91 \times 10^{-4}$	$5.92 \times 10^{-5}$
	InSb	$-4.48 \times 10^{-2}$	$+6.65 \times 10^{-2}$	$1.51 \times 10^{-2}$	$1.50 \times 10^{-2}$

**Table 3: Signal changes of the three different detector diodes extracted from Figures 1 to 3. The relative signal change was computed by normalizing the data to the mean and subtracting one. The root mean square (RMS) is shown for the raw data and after the exponential model has been subtracted.**

below  $5 \times 10^{-5}$  (0.005 %). At these levels there is probably a significant contribution originating from the finite resolution and/or slow update interval of the  $5\frac{1}{2}$  digit Picoammeter. This is illustrated in Fig. 4, where the residuals of the normalized diode signal after subtracting the best fit function show significant “banding”, meaning that the same diode current was recorded in the telemetry stream several times in a row.

The next question is whether the observed detector readings actually trace the light output of the RCSS lamp/filament. Given the fact that all three diodes show the same trend in basically all cases and are measured with independent Picoammeters, this is considered likely. It is also supported by the fact that even short term variations like the ones observed towards the end of the test in Fig. 1 can be seen in the Si and InGaAs diodes. If the source of these small variations is indeed the lamp itself, this is to be expected, since the wavelength coverage of those diodes overlap around the 0.9 micron region.

In addition, the relative magnitude of the drifts observed with the three diodes also support the lamp/filament as the source of the changes. The InSb diode shows by far the largest drifts, which can be explained by the fact that the lamp (and entire RCSS) slowly heats up when switched on. Since the bulb of the lamp is only partially transparent at wavelengths  $\lambda > 2.8 \mu\text{m}$ , the (relatively cold) bulb itself will emit in this wavelength region, and increasingly so when warming up. The changes observed with the Si and InGaAs diodes are believed to originate from small temperature changes of the filament itself. Here, the Si diode sees the stronger drift because it is mainly sensitive for wavelengths below  $0.9 \mu\text{m}$  and thus only covers the Wien part of the spectral energy distribution (SED) emitted by the filament<sup>1</sup>. The SED of the Wien part is highly dependent on the temperature of the emitting (grey) body, therefore even very small changes in temperature result in a significant change of the SED and thus the diode signal. For the InGaAs diode, the drift is smaller, because it covers a larger

<sup>1</sup>the filament runs at temperatures lower than 1900 K, thus the peak wavelength is around  $1.6 \mu\text{m}$



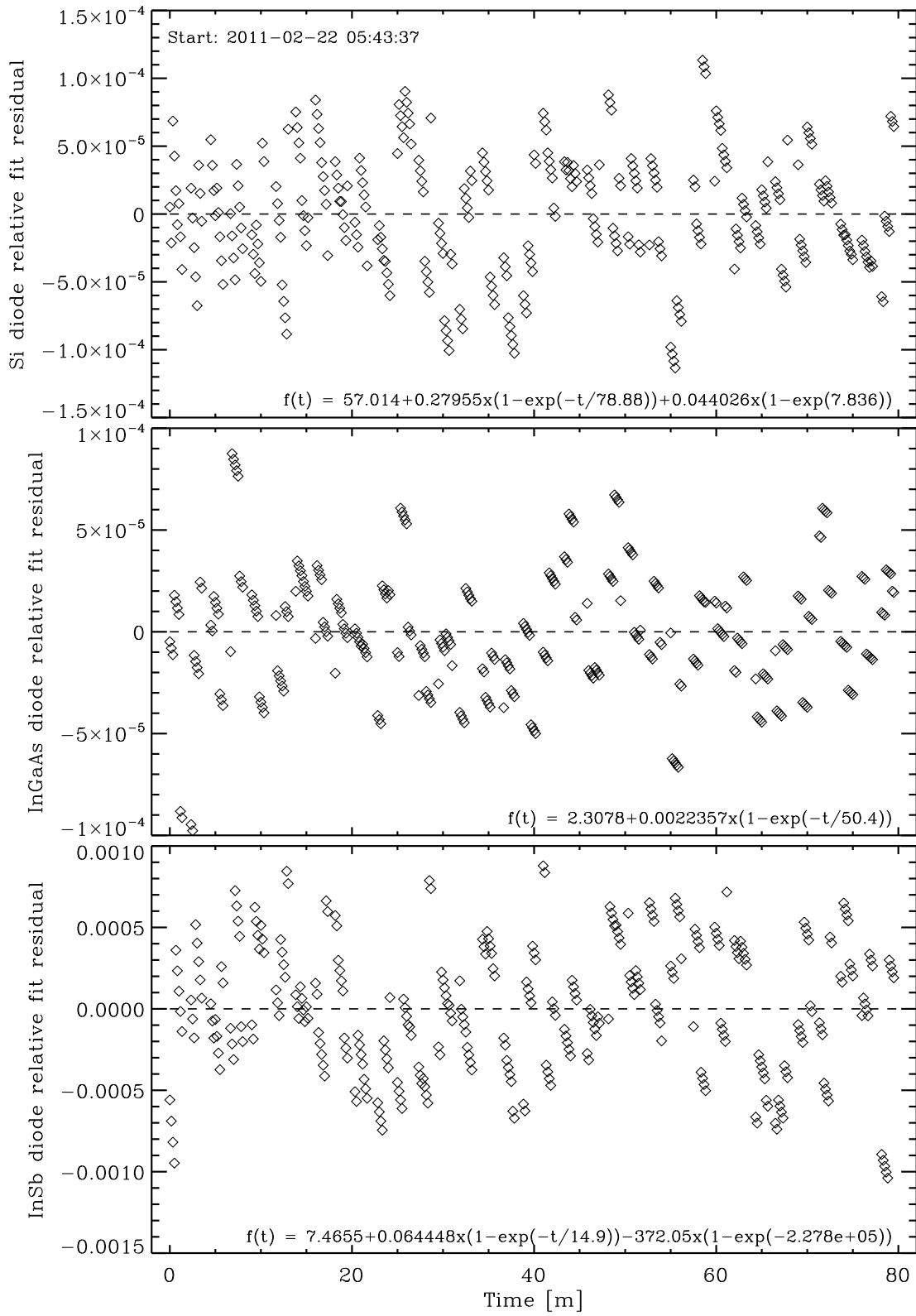


Figure 4: Relative fit residual of the three RCSS diodes with the data from Fig. 2.

wavelength range extending to  $1.9 \mu\text{m}$ , and thus beyond the peak of the SED, making it less sensitive to small temperature changes.

If we assume that the observed detector readings are indeed due to changes in the lamp and filament, and thus truly trace the output of the RCSS towards the NIRSpec instrument, the diode data can be used to correct for a significant fraction of the source drift when simulating exoplanet transit observations in the second NIRSpec calibration campaign.

## 4 SIMULATING EXOPLANET TRANSIT OBSERVATIONS

In this section, we briefly discuss which NIRSpec and RCSS configuration one should use when simulating exoplanet transit observations through the S1600 aperture. This assessment is based on the findings presented above and other constraints given by the nature of these observations: i) the spectrum shall cover both NIRSpec detectors and ii) the illuminating source of the spectrum shall be as bright as possible.

When covering both detectors with a spectrum originating from the same source (the RCSS), eventual drifts in the source should be seen in both detectors. On the other hand, if the drift is due to the NIRSpec SCAs, there is no reason why this drift should be correlated between the two detectors. Both SCAs see parts of the spectrum when using the high resolution gratings. Point two is due to the fact that one wants to accumulate as many electrons as possible. Furthermore, we want to use a representative sub-array and number of integrations per exposure. Together with the use of the high resolution gratings this implies a very bright source. Based on the results above, a brighter source does not seem to hurt the stability of the RCSS, apart from increased drifts in of the InSb diode where thermal heating contributes significantly. In fact, a higher signal even seems to improve the accuracy of the modeling using equation (1), as is evident in the smaller RMS values for the IFS1\_N and MOS1\_N tests. Therefore, we propose to use the IFS3\_N source for the exoplanet transit simulations, as it is the brightest RCSS source available (see table 1). Although it has not been used long enough in cycle 1 to assess its radiometric stability, we argue that its behavior should be similar to that of IFS1\_N and MOS1\_N, because the drive current to and the power dissipated by the filament is the same in all three cases, only the aperture towards the integrating sphere differs.

Regarding which high resolution grating of NIRSpec to choose, we propose to use the G140H Band I grating with the F100LP filter. This mode will cover the 1.0 to 1.8 micron range with NIRSpec, basically the same wavelength range where the InGaAs diode in the RCSS is most sensitive and the RCSS shows its best stability.

To summarize, we suggest that the exoplanet transit observation simulation is conducted using the G140H grating with the F100LP filter and the IFS3\_N RCSS lamp as point source, because it offers the most promising setup to characterize the stability of the NIRSpec detector system. This choice is not driven by the wavelength coverage needs of actual exoplanet transit observations. We do, however, expect that any findings regarding FPA stability will also apply to the other NIRSpec modes/dispersers.

## **5 REFERENCES**

Birkmann, S. 2011, Description of the NIRSpec optical ground support equipment (OGSE), NIRSpec Technical Note NTN-2011-002, ESA/ESTEC

Kochems, D. 2010, RCSS User Manual, User Manual NIRS-ASD-MA-0004, Astrium GmbH